CFA/VISHNO 2016

Approche ”fabless” de fabrication des micro-transducteurs électroacoustiques - Fabless Approach to the Fabrication of Electroacoustic Micro-transducers

L. Rufer
Univ. de Grenoble / Laboratoire TIMA, 46, Av. Felix Viallet, 38031 Grenoble, France
libor.rufer@imag.fr

LE MANS

Silicon-based microphones are nowadays well-established MEMS components produced by strong industrial actors. The fabrication of such acoustic sensors is based on a dedicated technology fulfilling all designed parameters. On the other hand, the development of such a technology processes is costly and time-consuming. In this paper, we will present a reversed approach, in which a device design must be tailored to match an existing fabrication process. We will show, on several examples, a design process of acoustic micro-transducers fabricated through a multi-projects wafer services. Focused will be a CMOS-MEMS process applied to the realization of suspended diaphragms that can be part of transducers with piezoresistive, electrostatic, or electrodynamic transduction. Obtained results will be presented, specific challenges and limitations of such a process will be discussed. Possible future solutions will be outlined.

1 Introduction

Various ways have been proposed since last two decades to fabricate suspended micro-structures based on a standard complementary metal oxide semiconductor (CMOS) process. The main benefit of this technique is that it can integrate micro-electro-mechanical systems (MEMS) and electrical circuits into a monolithic chip. This approach reduces parasitic effects between electromechanical devices and electrical circuits as well as the noise, which enhances the performance of these devices.

This, so called, CMOS-MEMS process was originally introduced as a technique using backside bulk micro machining (BSBM) and was applied in numerous designs [1]. Later, other approaches to CMOS-based MEMS fabrication using surface micromachining applied on specific layers issued from a CMOS process were proposed [2]. In one approach, keeping metal layers for a device design, a sacrificial silicon oxide can be removed with buffered oxide etch saturated with aluminum (SiloxVapox) [3]. In other approach, sacrificial metal layers can be etched with phosphoric, acetic and nitric acids. Remaining structure is then composed of silicon nitride, silicon oxide and polysilicon layers [4].

All these various CMOS-MEMS fabrication techniques are accessible through Multi-Projects Wafer (MPW) services as CMP (Circuits Multi-Projects) in France, Europractice IC in Germany, or MOSIS (MOS Implementation Service) in USA. A relatively easy execution and a moderate cost of MPW services present advantages for small companies and research institutions that have no access to a technology infrastructure necessary for MEMS-based devices development. This access can be used not only for a demonstrator design or a feasibility study but also for a final product fabrication in a fabless company model. A main inconvenient of the CMOS-MEMS approach resides in a fact that materials and their vertical dimensions available for a design work are strictly limited to those existing in a CMOS technology. This limitation can be overcome by using post-CMOS approaches that require some supplementary technology steps, like material deposition [5] or backside substrate etch [6], to build the entire MEMS structure.

Acoustic devices as microphones [6,7], CMUTs (capacitive micro-machined ultrasonic transducers) [5,8], or speakers [9] have been fabricated using various microtechnologies by various authors. In this paper, we will present our effort in the design of various types of acoustic devices based on CMOS-MEMS approach.

The paper is structured as follows. In Section 2, we will give an overview of the CMOS technologies and we will describe various approaches applied to the CMOS-MEMS techniques. In Section 3, we will present acoustic devices based on the CMOS-MEMS approach developed by our group. Finally, Section 4 will provide some conclusions and directions on our future research.

2 CMOS Technologies and MEMS

In this paragraph, we will present firstly a basic arrangement of a typical CMOS structure and then, we will describe approaches to the CMOS-MEMS fabrication.

2.1 CMOS Technology – Basis

Since its first announcement five decades ago, the CMOS technology, a major class of integrated circuits, is experiencing a sustainable evolution of its structure. A constant semiconductor process scaling, measured by the process node (transistor gate length) has decreased from 10 µm at 1971 to the actual value of 14 nm. The CMOS processes used extensively for the MEMS design have ranged from nodes 0.8 µm through 0.6 µm to 0.35 µm. These processes differ in term of the composition, number of layers deposited on the silicon substrate and their thicknesses. For the illustration, we show in Figure 1 the cross-section of a structure obtained by the AMS 0.35 µm CMOS process. The structure is composed of four metallization layers separated by four dielectric layers of silicon oxide. The passivation layer is deposited on top of the metallization layer M4.

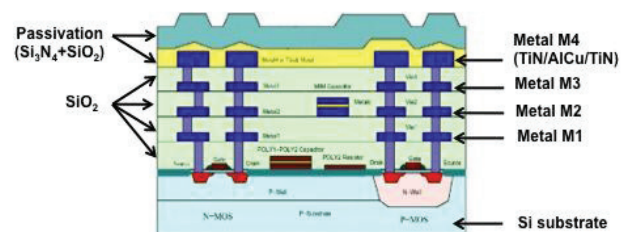

Figure 1: Cross-section of a structure obtained by the AMS 0.35 µm CMOS process.

From the perspective of microsystems, additional fabrication steps can be performed on a silicon wafer before (pre-CMOS), in-between, (intermediate-CMOS), or after (post-CMOS) regular CMOS steps.

Taking into account limits in terms of the compatibility of additional steps with the CMOS process, possible contamination, or communication with a foundry, the post-CMOS process is the most attractive one. Two fabrication strategies can be applied in the post-CMOS approach. The MEMS structure can be either built on top of a finished CMOS substrate, or obtained by its micromachining. In this case, the layers normally used for electrical interconnect can be appropriately patterned and applied as structural or transducer elements of a MEMS device. Two principal

approaches to the fabrication of freestanding microstructures, using either a bulk etching of the silicon substrate or a surface etching of certain CMOS layers on top of the wafer, will be described in the rest of this paragraph.

2.2 CMOS-MEMS with Si Bulk Etch

The first report of a technique allowing a fabrication of microstructures directly integrated in a standard CMOS process was given in [10]. In this work, a bulk etching of the silicon substrate is performed to obtain suspended structures composed of metallic and dielectric layers present on the substrate.

A silicon bulk etching can be applied either on the backside or on the front side of the wafer. The first solution results in sealed diaphragms (see Figure 2), but needs to use a whole wafer that permits an alignment of a mask with a structure designed as a diaphragm. The etching can be either isotropic or anisotropic, and typically, the first silicone oxide layer on the substrate is used as an inherent etch-stop.

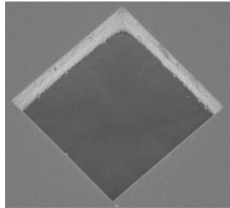

Figure 2: A diaphragm obtained by a backside isotropic etching of a silicon wafer.

Various structures, as cantilevers, bridges, or perforated diaphragms can be obtained after front-side silicon bulk etching. In this case, the passivation layer of silicon nitride is patterned and used as a mask. An advantage of this approach is that such a mask is prepared during the generation of the layout and the etching can be thus performed on a single chip.

2.3 CMOS-MEMS with Surface Etch

More recently, other approaches to a CMOS-based MEMS fabrication were proposed. These techniques are based on surface micromachining applied on specific layers issued from CMOS processes. Thus metallic layers can be considered as sacrificial ones and can be removed for instance with PAN etch (Phosphoric, acetic and nitric acids). Remaining structure is then composed of silicon nitride, silicon oxide and polysilicon layers [4].

In some cases, it is more convenient to keep metallic layers for device design. In this case, silicon oxide is chosen as a sacrificial layer and is removed for example with buffered oxide etch (BOE) saturated with aluminum (silox vapox III – Transene) [3]. Further, the silicon oxide can also be etched by vapor HF, which does not attack the aluminum layers and prevents inter-layers stiction.

The AMS 0.35 µm CMOS process presented in Figure 1 dispose of four metallic layers. In Figure 3a, these layers can be clearly distinguished after the etch of the sacrificial silicon oxide. If necessary, the metallic layers can be electrically connected through cylindrical blocks of tungsten (called 'vias') as shown in Figure 3b.

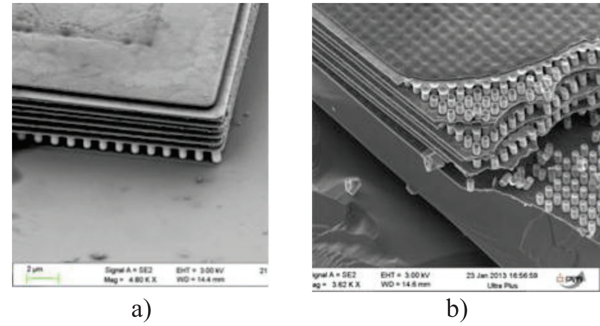

a) b)

Figure 3: Building elements of the CMOS-MEMS technology with the surface etching of the sacrificial layer of silicon oxide. (a) Metallic layers after the sacrificial silicon oxide etch; (b) view on the 'vias' structure that serves to interconnect metallic layers.

3 CMOS-MEMS Acoustic Devices

In this paragraph, we will present several acoustic devices designed based on the CMOS-MEMS approaches discussed in the previous paragraph.

3.1 Ultrasound Pulse-echo Device

An integrated micromachined ultrasound transducer (MUT) that can work as an emitter and a receiver of ultrasonic signals in air was designed and fabricated using a CMOS process combined with a backside silicon etching [11,12]. Among possible applications of the device there can be distance detection or measurements of different objects where the nature either of these objects or of their surroundings does not allow the use of light-based methods.

In the device are integrated, in a same chip, a suspended diaphragm and the associated interface electronics. The excitation of the diaphragm, and thus the ultrasound signal generation is based on the thermo-electrical effect; the sensing of the diaphragm deformation due to the ultrasound signal is achieved through a piezoresistive transduction. Four thermopiles (composed of polysilicon/aluminum thermocouples) are placed diagonally from the corners of the membrane towards its center. They serve the purpose of measuring the membrane temperature.

During emission, the diaphragm is thermally actuated at its resonant frequency (40 kHz) by a resistor placed at its center (Figure 4). During reception, a piezoresistive bridge placed on the diaphragm is used to monitor its deflection. Both the heating resistor and the piezoresistors are patterned in the polysilicon layer.

The fabrication of the system was done in two separate stages. In the first stage, the electronics section was fabricated and the diaphragm functional layers (resistor, piezoresistors and thermopile) were patterned by the standard 0.8 µm CMOS process. During this phase, a set of patterned layers of doped silicon, polysilicon, metal, silicon dioxide, and silicon nitride passivation is created on the wafer. These layers are used to form the electronic circuit and the diaphragm as well. The diaphragm is composed of the LOCOS layer (wet oxide), the gate oxide (dry oxide), the deposited interlevel oxides, and the silicon nitride passivation with a total thickness of 4.2 µm.

In the second stage of the fabrication process, the front side of the wafer was protected by a resist layer and the backside bulk micromachining process was used for the fabrication of the ultrasonic transducer. A Bosch DRIE

process commonly used to achieve deep anisotropic Si etching with high aspect ratio combined with high etch rate, high uniformity, and high mask selectivity has been applied. Figure 4b shows the result of the DRIE etch. We can see here the sidewalls of the silicon wafer through the optically transparent SiO_2 / Si_3N_4 diaphragm.

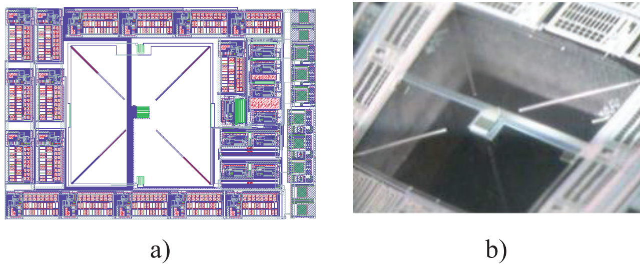

a) b)

Figure 4: (a) Layout of the complete device prepared for the AMS 0.35 µm CMOS process. (b) Micrograph of the diaphragm obtained by the DRIE etching.

The device was tested both in a generator and in a sensor mode. Figure 5a shows, as a function of frequency, the sound pressure level of the signal generated in a distance of 10mm from the diaphragm. The maximal pressure at the frequency of 41,2 kHz is equal to 35 mPa. Figure 5b shows the device output voltage corresponding to the sensitivity of 35 mV/Pa.

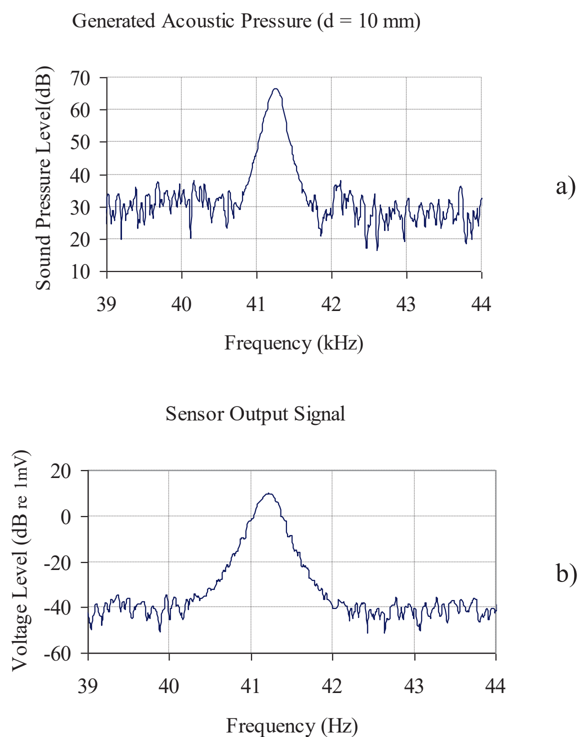

Figure 5: Measured results of the realized device in the mode of (a) generator; (b) sensor.

3.2 Electrodynamic Sensor

MEMS microphones or other acoustic sensors based on electrodynamic principle need to introduce a magnetic material that, typically, makes not a part of a typical fabrication process. An example of such a structure shown in [13] leads to relatively bulky device that cannot be considered for a batch microfabrication.

A technique of the silicon bulk etching applied on a front-side of a wafer was applied in the development of a CMOS-MEMS electrodynamic acoustic sensor [14,15]. A full CMOS compatibility of this design overcomes the technological handicap in terms of need of specific materials and fabrication technologies and allows a future monolithic integration of the sensor with its electronics using standard CMOS process.

The sensor consists mainly of two inductors, which occupy separate regions. The first one, a stationary outer inductor L_1, is placed on top of the substrate. The second one, an inner inductor L_2 is patterned on top of a thin plate suspended over a micromachined cavity. The plate is attached to the substrate using four crab-leg arms (see Figure 6a and serves as the sensor diaphragm. The electromagnetic field necessary for the sensor operation can be produced by an electrical bias applied in one or in both inductors. The bias can be insured either with a direct current (DC) or with an alternating current (AC). Thus, a magnetic field variable in space and/or in time will be generated in the vicinity of the inner inductor L_2. Figure 6a shows a simplified layout of both inductors, having only 5 turns as an example. Figure 6b shows in a schematic cross-section the interconnection of the inner end of the inner inductor L_2 with the contact pad through the metallic layer M1 and 'via' layer.

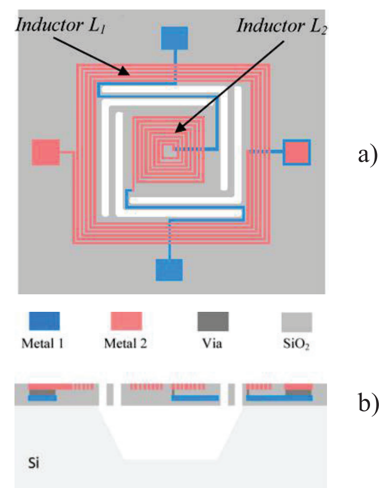

Figure 6: (a) Simplified layout of the sensor; (b) cross-section showing two metallic layers and 'via'.

The fabrication of the acoustic sensor is based on the AMS 0.6 µm CMOS process followed by an additional front-side bulk micromachining post-process to release both the diaphragm and its attachments. The micromachining involves a TMAH (tetramethylammonium hydroxide) wet etch that attacks only the bulk silicon and subsequently allows the etching of the cavity under the diaphragm.

The overall performance of the sensor depends on the size of the suspended diaphragm and is also influenced by the built-in stress, the bias voltage, and the cavity size. The sensitivity is mainly determined by the resonant structure, which is governed by the mass and the bending constant, and secondly by the damping which is a function of the airflow between the back chamber and the ambient air. From Figure 7, we note that when the air gap thickness increases, the whole circuit sensitivity also increases, but at the expense of the bandwidth.

It is useful to note that the induced voltage is inversely proportional to the average separation distance, ε_a, between L_1 and L_2. Consequently, both inductors should be placed as close as possible to maximize the output voltage. Moreover, the frequency of the electromotive force is

doubled compared to the incident wave pressure, resulting from the factor $\xi \times v$ (ξ … displacement, v … velocity), which is supposed as a serious weakness of the actual design. To deal with this problem, it can be shown that, for a given optimal diaphragm offset z_0, the induced voltage will only depend on the inductor geometrical parameters and diaphragm velocity, instead of a displacement-velocity product $\xi \times v$ [16].

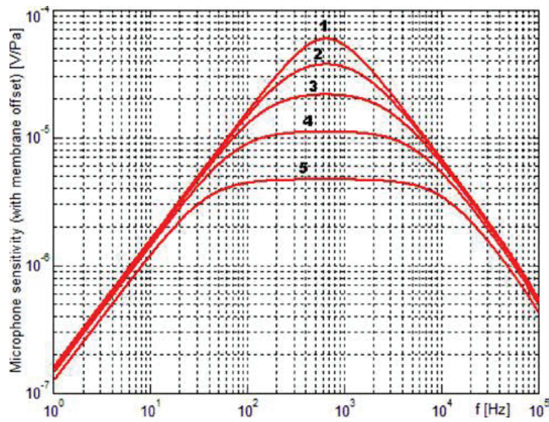

Figure 7: Microphone sensitivity as a function of the incident wave frequency for different values of the air-gap thickness g_0 (curves numbered from 1 to 5 correspond to descending values of g_0 from 70 µm to 30 µm).

3.3 Electrostatic Microphone

Various MEMS microphones have been developed by different groups and some designs, using dedicated technology process, have been commercialized until now. Most of the designs consist of movable electrode and a perforated fixed electrode, called the backplate, separated by an air gap (Figure 8). Below this backplate, there is a back-chamber that makes the evacuation of air from the air gap easier. The back-chamber is usually obtained by backside bulk micromachining.

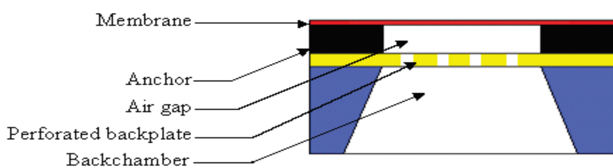

Figure 8: Schematic structure of a conventional MEMS condenser microphone.

In our work, we carry out a study and a development of a new concept of a condenser microphone [17,18,19]. This microphone structure does not contain a back-chamber, and is composed of a movable perforated electrode and a fixed electrode (with no holes), separated by an air gap (Figure 9). This kind of structure allows using of a standard CMOS process with only one additional post-process consisting in a sacrificial layers etching to realize the MEMS device. Holes dimensions and their position on the diaphragm have to be chosen to obtain a compromise between the etching time and the device acoustic performance. An important design effort is dedicated to the diaphragm perforation in order to avoid acoustic short-circuit in a low frequency range due to the acoustic pressure equalization.

Similar microphone structure with perforated movable electrode described in [20] used a specific dedicated technology to create an aluminum membrane. Moreover, the modeling does not take into account the air gap effect that is very important for the frequency response.

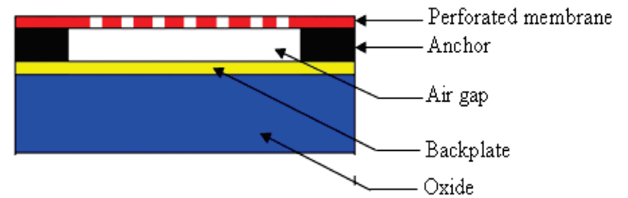

Figure 9: Schematic structure of a MEMS condenser microphone with a perforated membrane.

The microphone fabrication is based on AMS 0.35 µm CMOS back-end process that encompass a passivation layer, four metal layers, three via layers and several silicon dioxide layers. The Metal 4 layer is used for the diaphragm and Metal 2 layer for the backplate. The silicon dioxide layer between M4 and M2 is a sacrificial layer, which is removed by hydrofluoric acid (HF) wet or dry etching. The passivation layer has been opened at strategic places by AMS foundry (e.g. diaphragm, contacts for microphone).

We have focused on two different etching processes. One process used wet etching described in [3], based on HF solution SiloxVapox III (from Transene Company). We have obtained the etch rate for the silicon dioxide equal to 95 nm/min.

The second method is carried out with HF vapor etching using MONARCH-3 Primaxx from SPTS Company. The equipment has been designed especially for HF vapor etch to remove sacrificial silicon oxide layers, primarily to release microstructures in MEMS devices. Combining anhydrous HF vapor and alcohol vapor at reduced pressure and elevated temperature provides a wide, stable process window that can address different oxide compositions and thicknesses, while maintaining high selectivity to other common materials used in MEMS designs, including aluminum/alloy elements such as mirrors and bond pads [21]. MONARCH-3 is a compact module including a three-wafer process chamber, and is designed for research laboratories and small volume production environments. SEM pictures of one test structure (Figure 10) show that SiO_2 was completely removed after HF vapor etching. The etch rate has been estimated at 140 nm/min.

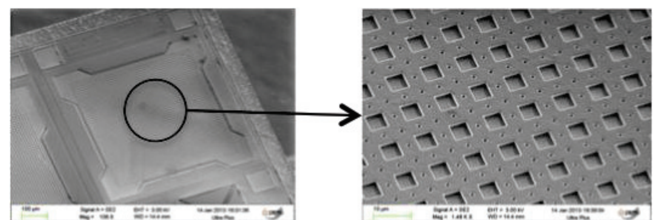

Figure 10: Schematic structure of a conventional MEMS condenser microphone.

We have performed some preliminary electrical and mechanical characterization of the test structures. The curve of Figure 11a shows the capacitance dependence on the polarization voltage. Figure 11b shows results of the measurements performed with an optical interferometer microscope (Fogale Nanotech) based on non-contact optical interferometry.

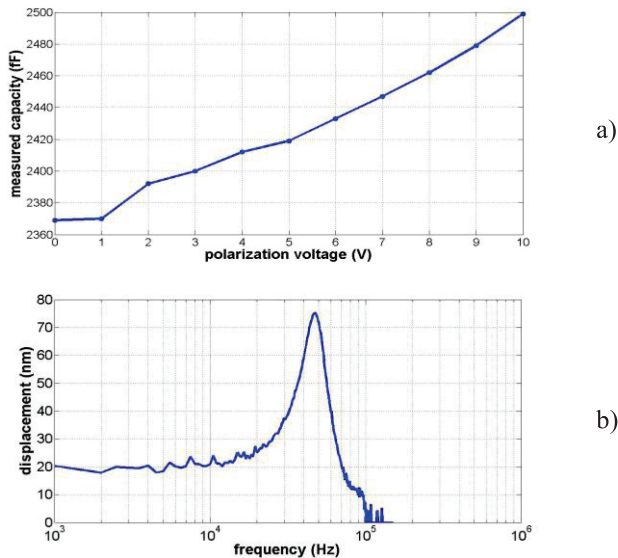

Figure 11: Characterization results of the microphone structure: (a) capacitance as a function of the polarization voltage; (b) diaphragm displacement as a function of frequency.

3.4 Acoustic Micro-source

A successful design of an efficient source generating acoustic pressure in the air by means of vibrating diaphragm must maximize the product of the diaphragm area, its vibrational velocity and frequency. Such a condition limits the exploitation of MEMS-based devices as acoustic sources, in particular in low frequency range, to in-ear or similar applications generating low power signals in closed couplers. Various approaches to the acoustic generation in air with MEMS use magnetic or piezoelectric materials. Their principal disadvantage is the need to integrate a material that is not a part of a CMOS fabrication process. Another approach consists in digital sound reconstruction involving the summation of discrete acoustic pulses generated by individual acoustic transducers arranged in a matrix and operating in a binary way. Such a digital speaker was presented in a configuration using a capacitive principle [22]. Modeling methods of electrostatic MEMS micro-speakers were presented in [23]. CMOS-MEMS process with front-side surface etching of layers deposited on silicon wafer during the CMOS process presented in previous Paragraph can be considered for acoustic sources. Indeed, until now, various applications of this technology were reported except acoustic sources [24].

We have shown that the industrial 0.35µm CMOS technology can be considered also for sources of airborne acoustic signals [25]. The ultimate goal is the monolithic integration of a device working both as a source and a sensor with electronics, thus facilitating signal routing, suppressing parasitic effects, and improving the signal-to-noise ratio.

The acoustic source is based on the same structure as described in Paragraph 3.3. In order to estimate the available acoustic pressure generated by the structure, we have built its numerical model in the ANSYS environment. The model does not take into account the holes of the real device and the damping effects induced by the air gap and holes in the diaphragm were evaluated by a simultaneous fluidic analysis expressed by a global damping coefficient considered in the structural model. There are two elements involved in the simulations: the four-node structural shell element SHELL181 and the electromechanical transducer element TRANS126. With the maximal displacement obtained from the harmonic simulation, we can estimate the maximal acoustic pressure from the following expression:

$$p = \frac{\rho \, \pi \, f \, v \, a^2}{r}.$$

In this expression, considering the case of the piston–like movement and the far field, ρ is the density of the air, f is the frequency, v is the piston speed, a is the radius of the piston and r is the distance from the piston. Considering the displacement obtained at the natural frequency and converting it in an equivalent displacement related to the case of a piston–like movement, the estimated maximal pressure at *10 mm* from the plate is *20.2 mPa*.

The acoustic source was characterized with the acoustic measurement chain (microphone B&K 4939, lock-in amplifier Zurich Instruments HF2LI - Figure 12). Figure 13 shows the frequency response of the acoustic pressure generated by the MEMS device. With the DC bias of *8 V* and the AC actuation voltage of *6 V*, we have obtained at a distance of *10 mm* the maximal acoustic pressure of *12 mPa*.

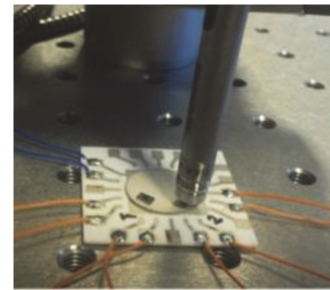

Figure 12: Part of the measurement setup for acoustic detection.

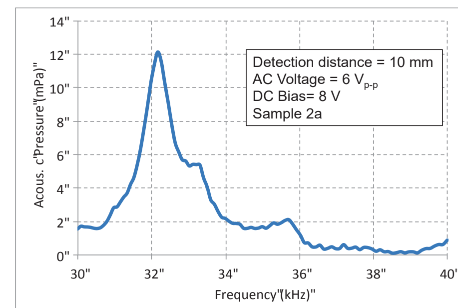

Figure 13: Frequency response of the CMOS-MEMS acoustic source.

4 Conclusion

We have presented in this paper several acoustic devices fabricated with various approaches based on standard CMOS technology. The presented examples confirm that both acoustic sensors and actuators can be designed for a technology that requires only one additional post-CMOS step. Such completely CMOS compatible approach can be easily combined with electronics on a same chip and result in an integrated device. Future work must be focused on the efficiency gain due to diaphragm openings optimization.

Remerciements

The work presented in this paper was developed during the PhD projects of Christian Domingues, Farès Tounsi, and Josué Esteves.

References

[1] Reay, R.L., Klaassen, E.H., Kovacs, G.T.A., Thermally and electrically isolated single crystal silicon structures in CMOS technology, IEEE Electron Device Letters, Vol. 15, 1994, pp. 399-401.

[2] Fedder, G.K., Santhanam, S., Reed, M.L., Eagle, S.C., Gulliou, D.F., Lu, M.S.C., Carley, L.R., Laminated high-aspect-ratio microstructures in a conventional CMOS process, *Sensors and Actuators A*, Vol. 57, 1996, pp. 103–110.

[3] Dai, C. L., A maskless wet etching silicon dioxide post CMOS process and its application, *Microelectronic Engineering*, Vol. 83, 2006, pp. 2543-2550.

[4] Chen, M-H., Lu, M.S-C., Design and characterization of an air-coupled capacitive ultrasonic sensor fabricated in a CMOS process, *J. of Micromechanics and Microengineering,* Vol. 18, 2008, 6 pp.

[5] Po-Kai Tang and al., Design and characterization of the immersion-type capacitive ultrasonic sensors fabricated in a CMOS process, *J. of Micromechanics and Microengineering*, Vol. 21, No. 2, 2011, 8 pp.

[6] Chien-Hsin Huang and al., Implementation of the CMOS MEMS Condenser Microphone with Corrugated Metal Diaphragm and Silicon Back-Plate, *Sensors* Vol. 11, No. 6, 2011, pp. 6257-6269.

[7] M. Pedersen, W. Olthuis, and P. Bergveld, High performance condenser microphone with fully integrated CMOS amplifier and DC-DC voltage converter, *J. of Microelectromechanical Systems*, Vol. 7, No. 4, 1998, pp. 387-394.

[8] Ergun, A.S., Huang, Y., Zhuang, X., Oralkan, Å, Yaralıoglu, G.G., and Khuri-Yakub, B.T., Capacitive Micromachined Ultrasonic Transducers: Fabrication Technology, *IEEE Transactions on Ultrasonics, Ferroelectrics, and Frequency Control*, Vol. 52, No. 12, December 2005, pp. 2242-2257.

[9] Shahosseini, I., Lefeuvre, E., Moulin, J., Woytasik, M., Martincic, E., Pillonnet, G., Lemarquand, G., Electromagnetic MEMS microspeaker for portable electronic devices, *Microsystems Technology*, Vol. 19, 2013, pp. 879–886

[10] Parameswaran, M., Baltes, H. P., Ristic, L., Dhaded, A. C., and Robinson, A. M. A new approach for the fabrication of micromechanical structures, *Sensors and Actuators A*, Vol. 19, No. 3, 1989, pp. 289-307.

[11] Domingues, C., Conception de transducteurs acoustiques micro-usinés, Ph.D. dissertation, National Polytechnic Inst., Grenoble, France, 2005, pp. 155.

[12] Rufer, L., Domingues, C., Mir S., Petrini, V., Jeannot, J.-C., Delobelle, P., A CMOS compatible ultrasonic transducer fabricated with deep reactive ion etching, *IEEE J. of Microelectromechanical Systems*, Vol. 15, No. 6, 2006, pp. 1766-1776.

[13] Horng, R.H., Chen, K.F., Tsai, Y.C., Suen, C.Y, Chang, C.C., Fabrication of a dual-planar-coil dynamic microphone by MEMS techniques, *J. of Micromechanics and Microengineering,* Vol. 20, 2010, pp. 1–7.

[14] Tounsi, F., Microphone électrodynamique MEMS en technologie CMOS : étude, modélisation et réalisation Ph.D. dissertation, University of Grenoble, France, 2010, pp. 135.

[15] Tounsi, F., Mezghani, B., Rufer, L., Masmoudi, M., Electroacoustic Analysis of a Controlled Damping Planar CMOS-MEMS Electrodynamic Microphone, *Archives of Acoustics*, Vol. 40, No. 4, 2015, pp. 527-537.

[16] Tounsi, F., Said, M.H., Rufer, L., Mezghani, B., Masmoudi, M., Induced Voltage Correction and Optimization of Coaxial-Planar-Inductances CMOS-Compatible MEMS Dynamic Microphones, *IEEE Sensors Journal*, under review.

[17] Esteves, J., Technologie CMOS-MEMS pour des applications acoustiques, Ph.D. dissertation, University of Grenoble, France, 2013, pp. 265.

[18] Esteves, J., Rufer, L., Basrour, S., Ekeom, D., CMOS-MEMS technology with front-end surface etching of sacrificial SiO_2 dedicated for acoustic devices, 5th IEEE International Workshop on Advances in Sensors and Interfaces (IWASI'13), Bari, Italy, 13-14 June 2013, pp. 154-159.

[19] Esteves, J., Rufer, L., Rehder, G., Capacitive Microphone fabricated with CMOS-MEMS Surface-Micromachining Technology, *Symp. on Design, Test, Integration and Packaging of MEMS/MOEMS,* Aix-en Provence, France, May 11-13, 2011, pp. 309-314.

[20] Ganji, B.A., Majlis, B.Y;, Design and fabrication of a new MEMS capacitive microphone using perforated diaphragm, *Sensors and Actuators A*, Vol. 149, 2009, pp. 29-37.

[21] http://www.spts.com/products/release-etch.

[22] Diamond, B. M., Neumann, J. J., Gabriel, K. J., Digital sound reconstruction using arrays of CMOS-MEMS microspeakers, Proc. Transducers '03, Boston, June 8-12, 2003, pp. 238-241.

[23] Tumpold, D., Kaltenbacher, M., Glacer, C., Nawaz, M., Dehé, A., Modeling methods of MEMS micro-speaker with electrostatic working principle, Proc. of SPIE 8763, 2013, pp. 1-12.

[24] Tang, P.K., Wang, P.H., Li, M.L., Lu, M.S.C., Design and characterization of the immersion-type capacitive ultrasonic sensors fabricated in a CMOS process, *J. Micromechanics and Microengineering,* Vol. 21, 2011, pp. 1-8.

[25] Rufer, L., De Pasquale, G., Esteves, J., Basrour, S., Somà, A., Micro-Acoustic source for Hearing Applications fabricated with 0.35µm CMOS-MEMS process, Eurosensors XXIX, September 6-9, 2015, Freiburg, Germany.